TECHNICAL NOTE

Real-Time FORC (RTForc™) Software for the 8600 Series VSM

B. C. Dodrill, H. S. Reichard, and T. Shimizu, Lake Shore Cryotronics

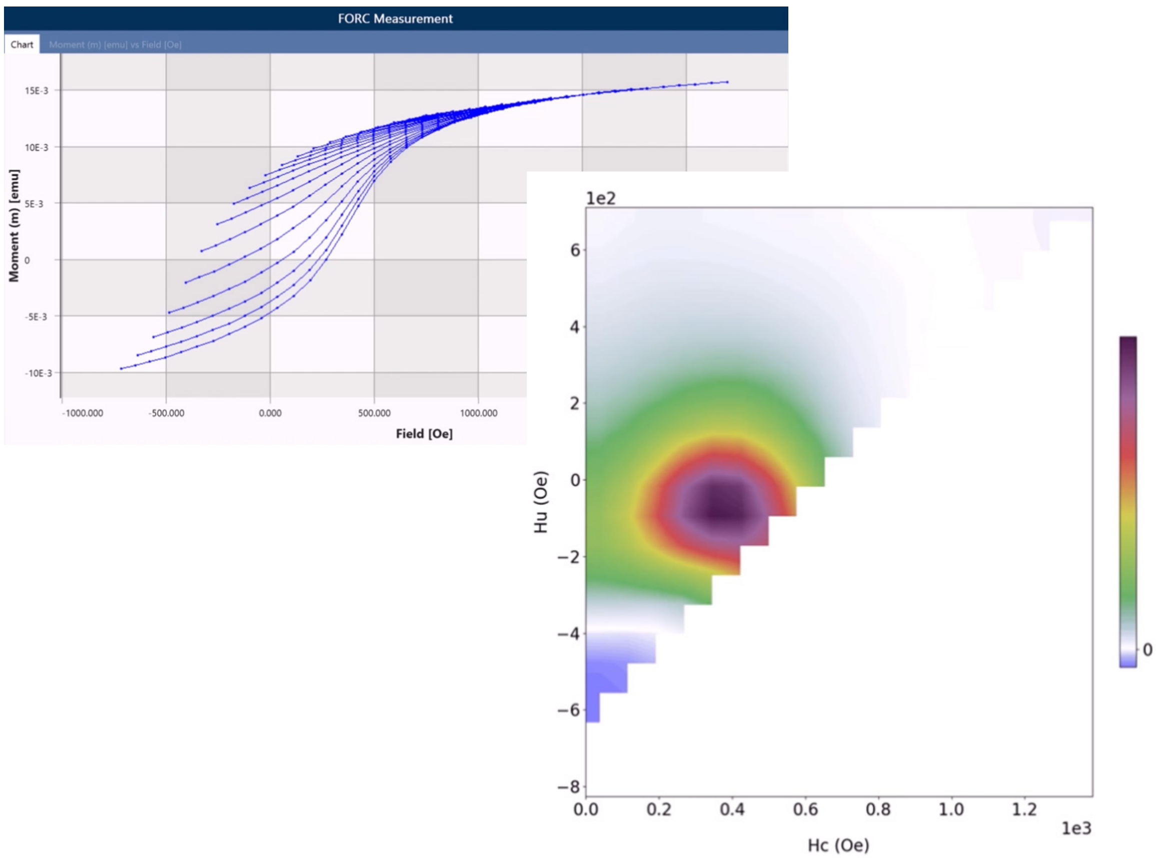

Key Features

- Fully automated FORC data acquisition using the 8600 VSM software
- FORC distributions are calculated and displayed in real-time, significantly reducing the time required to collect and analyze FORC data
- Users can change between the (H_a, H_b) and (H_c, H_u) coordinate systems, select smoothing factors (SF) and number of contours to be displayed, export the FORC diagram image, etc.
- Output data is compatible with FORCinel post-processing software

Lake Shore CRYOTRONICS

Background

First-order-reversal-curve (FORC) measurements and analysis provide information regarding magnetic reversal mechanisms in magnetic materials that cannot be obtained from major hysteresis loop measurements alone. It has been extensively used by earth and planetary scientists studying the magnetic properties of natural samples (rocks, soils, sediments, etc.) because FORC can distinguish between single-domain (SD), multi-domain (MD), and pseudo single-domain (PSD) behavior, and because it can discriminate between different magnetic mineral species[1, 2]. It has proven to be useful in better understanding the nature of magnetization reversal and interactions in magnetic nanowires[3 – 7], nanomagnet arrays[8 – 11], thin film magnetic recording media[12 – 14] and thin film magnetic multilayers[15 – 17], nanostructured permanent magnet materials[18,19], soft magnetic bilayers[20] and magneto-caloric effect (MCE) materials[21]. It has also been used to differentiate between phases in multiphase magnetic materials because it is very difficult to unravel the complex magnetic signatures of such materials from a hysteresis loop measurement alone[22 - 24].

A FORC is measured by saturating a sample in a field H_{sat}, decreasing the field to a reversal field H_a, then measuring moment versus field H_b as the field is swept back to H_{sat}. This process is repeated for many values of H_a, yielding a series of FORCs as shown in figure 1 for a magnetic tape. The FORC distribution $\rho(H_a, H_b)$ is the mixed second derivative:

$$\rho(H_a, H_b) = -(1/2)\partial^2 M(H_a, H_b)/\partial H_a \partial H_b$$

A FORC diagram is a 2D or 3D contour plot of $\rho(H_a, H_b)$. It is common to change the coordinates from (H_a, H_b) to:

$$H_c = (H_b - H_a)/2,\ H_u = (H_b + H_a)/2$$

H_u represents the distribution of interaction or reversal fields, and H_c represents the distribution of switching or coercive fields. The 2D FORC diagram for the magnetic tape is shown in figure 2.

A FORC diagram not only provides information regarding the distribution of interaction and switching fields, but also serves as a “fingerprint” that gives insight into the domain state and nature of interactions occurring in magnetic materials. In a FORC diagram entirely closed contours are usually associated with SD behavior, while open contours that diverge towards the H_u axis are associated with MD, and open and closed contours together are associated with PSD. The peak in the FORC distribution is usually centered at a switching field H_c that correlates with the coercivity as determined from a hysteresis loop measurement. If the peak in the FORC distribution is centered at an interaction field $H_u = 0$ this means that interactions are weak. Conversely, if the peak is shifted towards positive H_u they are strong. Multiple peaks in a FORC diagram mean there are multiple magnetic phases in a material. And the very shape of the FORC distribution provides insight into the nature of interactions (dipolar, exchange) that are occurring in a magnetic material.

The use of RTForc™ for FORC measurements

Conducting FORC measurements and analysis is usually an iterative process whereby one defines the FORC data acquisition parameters (figure 3 shows an example FORC Measurement setup), conducts the measurement, and then processes the data to generate a FORC diagram using 3rd party software (e.g., FORCinel[25], VARIFORC[26]). After the first FORC measurement, adjustments are often made to the FORC acquisition parameters and the sample is re-measured to better optimize the FORC diagram, e.g., (H_c, H_u) range, resolution, etc. Since FORC measurements can take tens of minutes to several hours or longer (depending on the density of data being collected, and the sample being measured), the time required to produce the desired FORC diagram can be quite long. Real-time FORC generates the FORC diagram as data is being collected, enabling one to easily see if FORC parameters were defined correctly, and thus significantly reduces the amount of time required to optimally collect and analyze FORC data.

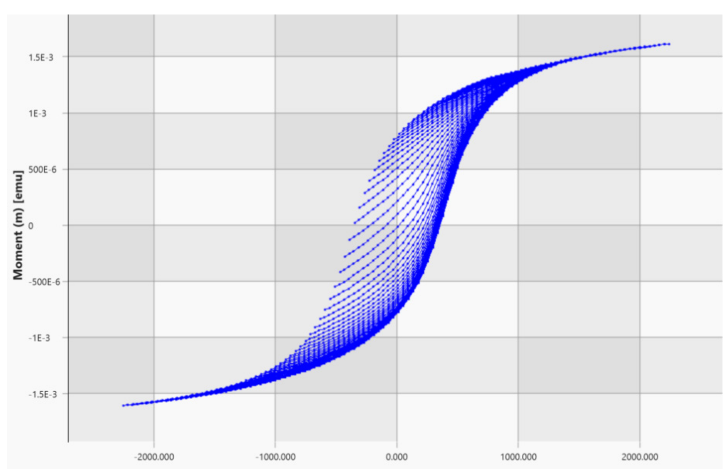

Figure 1: Measured FORCs for a magnetic tape.

Example RTForc diagrams:

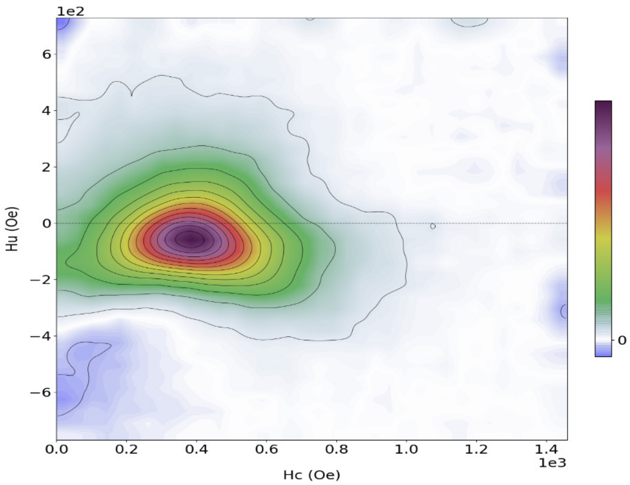

Figure 2: RTForc diagram for the magnetic tape. The peak is centered at H_c which correlates with the coercivity of the sample as determined from a hysteresis loop measurement. The peak is shifted towards negative interaction fields H_u and the distribution has a "boomerang" shape. These are features that are usually associated with exchange interactions.

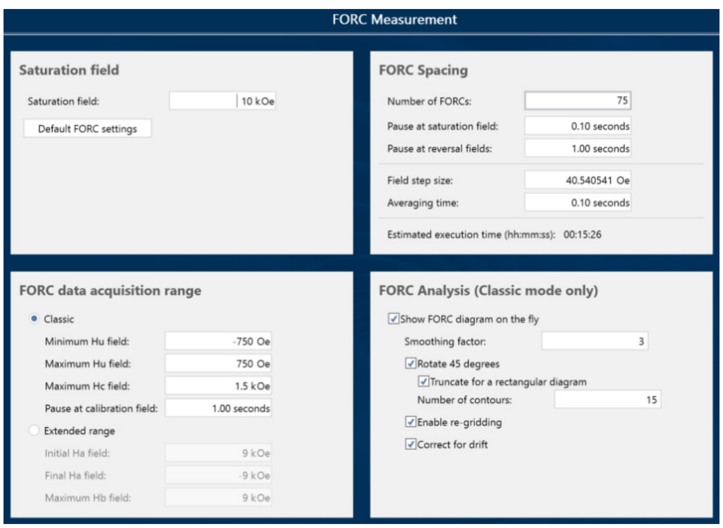

Figure 3: Example 8600 VSM FORC Measurement setup.

Watch a video demonstrating an RTForc™ measurement

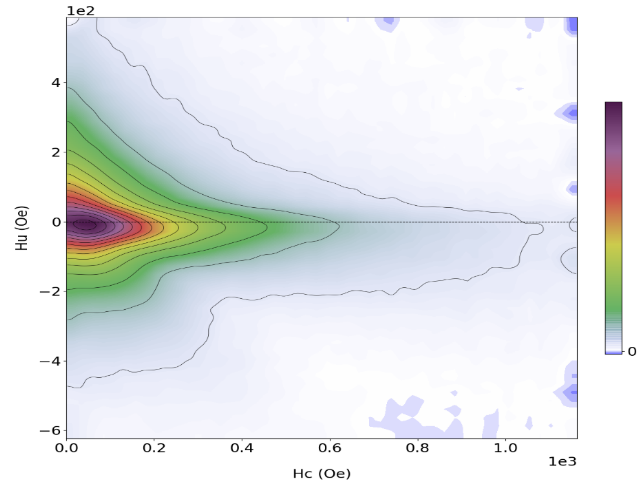

Figure 4: RTForc diagram for a marine sediment sample. The FORC diagram consists of both closed and open contours, the latter diverging towards the H_u axis. These features are usually associated with pseudo-single domain (PSD) behavior.

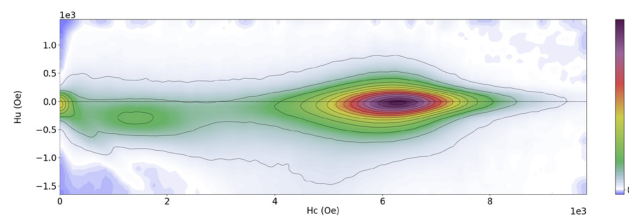

Figure 5: RTForc diagram for a $BaFe_{12}O_{19}$ nanoparticles (NP) sample. There are two peaks corresponding to low (soft) and high (hard) coercivity components, and the region between the two peaks is related to the exchange coupling between the two phases[24].

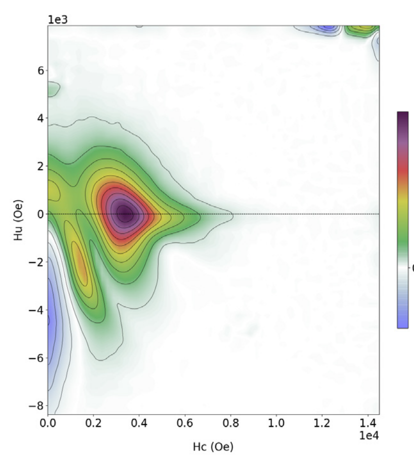

Figure 6: RTForc diagram for a permanent magnet sample. The FORC diagram has a "wishbone" like feature which is usually associated with long-range magneto-static (dipolar) interactions.

References:

1. C. R. Pike, A. P. Roberts, and K. L. Verosub, Characterizing Interactions in Fine Magnetic Particle Systems Using First Order Reversal Curves, J. Appl. Phys., 85, 6660,1999.

2. A. P. Roberts, C. R. Pike, and K. L. Verosub, First-Order Reversal Curve Diagrams: A New Tool for Characterizing the Magnetic Properties of Natural Samples, J. Geophys. Res., 105, 461, 2000.

3. A. Rotaru, J. Lim, D. Lenormand, A. Diaconu, J. Wiley, P. Postolache, A. Stancu, and L. Spinu, Interactions and Reversal Field Memory in Complex Magnetic Nanowire Arrays, Phys. Rev. B, 84, 13, 134431, 2011.

4. O. Trusca, D. Cimpoesu, J. Lim, X, Zhang, J. Wiley, A. Diaconu, I. Dumitru, A. Stancu, and L. Spinu, Interaction Effects in Ni Nanowire Arrays, IEEE Trans. Mag., 44, 11, 2730, 2008.

5. A. Arefpour, M. Almasi-Kashi, A. Ramazani, and E. Golafshan, The Investigation of Perpendicular Anisotropy of Ternary Alloy Magnetic Nanowire Arrays Using First Order Reversal Curves, J. Alloys and Comp., 583, 340, 2014.

6. B. C. Dodrill, and L. Spinu, First-Order-Reversal-Curve Analysis of Nanoscale Magnetic Materials, Technical Proceedings of the 2014 NSTI Nanotechnology Conference and Exposition, CRC Press, 2014.

7. A. Sharma, M. DiVito, D. Shore, A. Block, K. Pollock, P. Solheid, J. Feinberg, J. Modiano, C. Lam, A, Hubel, and B. Stadler, Alignment of Collagen Matrices Using Magnetic Nanowires and Magnetic Barcode Readout Using First Order Reversal Curves (FORC), J. Mag. Mag. Mat., 459, 176, 2018.

8. F. Beron, L. Carignan, D. Menard, and A. Yelon, Extracting Individual Properties from Global Behavior: First Order Reversal Curve Method Applied to Magnetic Nanowire Arrays, Electrodeposited Nanowires and Their Applications, edited by N. Lupu, 228, INTECH, Croatia, 2010.

9. R. Dumas, C. Li, I. Roshchin, I. Schuller, and K. Liu, Magnetic Fingerprints of sub-100 nm Fe Nanodots, Phys, Rev. B, 75,134405, 2007.

10. D. Gilbert, G. Zimanyi, R. Dumas, M. Winklhofer, A. Gomez, N. Eibagi, J. Vincent, and K. Liu, Quantitative Decoding of Interactions in Tunable Nanomagnet Arrays, Sci. Reports, 4, 4204, 2014.

11. J. Graffe, M. Weigand, C. Stahl, N. Trager, M. Kopp, G. Schutz, and E. Goering, Combined First Order Reversal Curve and X-ray Microscopy Investigation of Magnetization Reversal Mechanisms in Hexagonal Antidot Arrays, Phys. Rev. B, 93, 014406, 2016.

12. B. Valcu, D. Gilbert, and K. Liu, Fingerprinting Inhomegeneities in Recording Media Using First Order Reversal Curves, IEEE Trans. Mag., 47, 2988, 2011.

13. A. Stancu and E. Macsim, Interaction Field Distribution in Longitudinal and Perpendicular Structured Particulate Media, IEEE Trans. Mag., 42, 10, 3162, 2006.

14. M. Winklhofer, R. K. Dumas, and K. Liu, Identifying Reversible and Irreversible Magnetization Changes in Prototype Patterned Media Using First- and Second-Order Reversal Curves, J. Appl. Phys., 103, 07C518, 2008.

15. R. Dumas, C. Li, L. Roshchin, I. Schuller, and K. Liu, Deconvoluting Reversal Modes in Exchange Biased Nanodots, Phys. Rev. B, 144410, 2012.

16. R. Gallardo, S. Khanai, J. Vargas, L. Spinu, C. Ross, and C. Garcia, Angular Dependent FORC and FMR of Exchange Biased NiFe Multilayer Films, J. Phys. D: Appl. Phys., 50, 075002, 2017.

17. N. Siadou, M. Androutsopoulos, I. Panagiotopoulos, L. Stoleriu, A. Stancu, T. Bakas, and V. Alexandrakis, Magnetization Reversal in $[Ni/Pt]_6/Pt(x)/[Co/Pt]_6$ Multilayers, J. Mag. Mag. Mat., 323, 12, 1671, 2011.

18. T. Schrefl, T. Shoji, M. Winklhofer, H. Oezeit, M. Yano, and G. Zimanyi, First Order Reversal Curve Studies of Permanent Magnets, J. Appl. Phys., 111, 07A728, 2012.

19. M. Pan, P. Shang, H. Ge, N. Yu, and Q. Wu, First Order Reversal Curve Analysis of Exchange Coupled SmCo/NdFeB Nanocomposite Alloys, J. Mag. Mag. Mat., 361, 219, 2014.

20. M. Rivas, J. Garcia, I. Skorvanek, J. Marcin. P. Svec, and P. Gorria, Magnetostatic Interaction in Soft Magnetic Bilayer Ribbons Unambiguously Identified by First Order Reversal Curve Analysis, Appl. Phys. Letts., 107, 132403, 2015.

21. V. Franco, F. Beron. K. Pirota, M. Knobel, and M. Willard, Characterization of Magnetic Interactions of Multiphase Magnetocaloric Materials using First Order Reversal Curve Analysis, J. Appl. Phys., 117, 17C124, 2015.

22. B. C. Dodrill, First-Order-Reversal-Curve Analysis of Nanocomposite Permanent Magnets, Technical Proceedings of the 2015 TechConnect World Innovation Conference and Expo, CRC Press, 2015.

23. C. Carvallo, A. R. Muxworthy, and D. J. Dunlop, First-Order-Reversal-Curve (FORC) Diagrams of Magnetic Mixtures: Micromagnetic Models and Measurements, Physics of the Earth and Planetary Interiors, 154, 308, 2006.

24. Y. Cao, M. Ahmadzadeh, K. Xe, B. Dodrill, and J. McCloy, Multiphase Magnetic Systems: Measurement and Simulation, J. Appl. Phys., 123(2), 023902, 2018.

25. R. J. Harrison and J. M. Feinberg, FORCinel: An Improved Algorithm for Calculating First-Order Reversal Curve Distributions Using Locally Weighted Regression Smoothing, Geochemistry, Geophysics, Geosystems, 9, 11, 2008.

26. R. Egli, VARIFORC: An Optimized Protocol for Calculating Non-regular First-Order Reversal Curve (FORC) Diagrams, Global and Planetary Change, 203, 110, 203, 2013.